Design of Miniaturized Microwave Filtering-Balun Component for Wireless Applications

Haider Zwain[1,*], and *Naser* Alkhafaji[2]
[1] Communication Engineering Department, Al-Furat Al-Awsat Technical University, Technical Engineering College of Najaf

[2] Laser and Optoelectronics Engineering Department, Al-Furat Al-Awsat Technical University, Technical Engineering College of Najaf

Abstract. This research paper introduces a new design being Minkowski-like fractal filtering-balun MLFFB based on the dual-mode ring resonator. The structure has three ports, converting the signal from one unbalanced port to two balanced ports (i.e., 180° phase shift). The proposed design can act as a filter and balun simultaneously using one dual-mode ring resonator. The fractal curves are applied to have compact designs. The 0th, 1st, and 2nd iterations of the Minkowski-like fractal curves are applied to demonstrate the miniaturization ratio obtained in the proposed work. The miniaturization ratios are 47.8% and 73% of the 1st iteration and 2nd iteration of the Minkowski balun-filtering components, respectively, compared to the 0th iteration. Also, the filtering balun has a distinctive feature, which is the control of the phase error and magnitude imbalance of the two balanced ports, depending on the size of the perturbation part. Several structures have been designed, modeled, and analyzed utilizing the Advanced Design System (ADS) software. Each design iteration is evaluated and optimized to attain the best performance. The operating frequency is 2.4 GHz, and the realized transmission coefficients are S_{21} = -7 dB and S31 = -6.5 dB, which are less than expected ideal values because the substrate is a lossy type, being FR4. The S_{11} is less than -10 dB. The proposed design is a good candidate for narrow-band wireless applications.

1 Introduction

Nowadays, wireless communication systems dominate almost all daily life applications, and they have become an essential part of everything, especially when Internet-of-Things (IoT) technology has emerged. The systems can cover different functions in one device, like communication, global positioning systems (GPS, Wi-Fi, Bluetooth), devised connections, etc. Thus, each function requires its own RF chain, leading to a complicated design. However, designers always seek to find a method to combine several components in one design for many reasons, such as small size and low cost. In this research, the proposed RF component functions as a filter and a balun simultaneously in one RF component. The dual-mode ring resonator is a milestone in the research.

The dual-mode ring resonator plays a vital role in several RF and optical applications, such as microwave filters [1-3], baluns [4-5], oscillators [6], sensors [7-8], unit cells of metamaterial devices [9–10], optical filters [11], and microwave multiplexers [12]. In this introduction, only the filters and baluns will be reviewed.

*Corresponding author: haider.ms.etcn25@student.atu.edu.iq

In their earliest work, the authors of [1–2] used the ring resonator to act as a microwave bandpass filter for the first time. Their works focused on how to excite the two modes by perturbing the modes using the patch stub. In [3], the author presented a comprehensive work about using the ring resonator in the filter design. Different arrangements of perturbations were investigated to see their effect on the overall performance. The inductive and capacitive couplings,depending on the perturbation size, were defined. The capacitive coupling excites a response with an elliptical transfer characteristic, while the inductive coupling has a Chebyshev transfer response. The former introduces zeros in the response, so its selectivity is high. The latter one has no zeros, so its selectiveness is lower. However, there is no ripple in the passband. These two fascinating works attracted a lot of researchers to pursue studying ring resonators and their applications. The four sides of the dual-mode ring resonators have regions with maximum fields but with different phases, so these inherent characteristics aided in designing a balun as in [4–5]. The difference between the filter and balun when utilizing the ring resonator is the process of adding a third port. Moreover, the ring resonator balun offers bandpass filter characteristics, so two functions are combined in one design structure. Then, many research efforts have emerged, and one of these things is miniaturization. In [13–15], authors used fractal geometry to develop small dual-mode ring resonators-based designs of microwave bandpass filters, where Minkowski, Koch, Gasket, and other curves were employed.

The fractal curves were also used in the Balun design but using an open-loop resonator [16–17]. The Koch-fractal type was used. The main key difference between the open loop and dual-mode ring resonator is that the latter has the property to control the bandwidth by altering the perturbation size, so the latter is adopted here in this research. To miniaturize the microwave filtering-balun structure based on the dual-mode ring resonator, the fractal curves will be applied for the first time according to the best of the authors' knowledge.

This paper is organized as follows: in Section II, the proposed filtering-balun configuration is presented. Section III introduces the filtering-balun design. Next, Section IV provides a detailed discussion about the obtained results. Finally, the conclusion is drawn.

2 The Proposed Filtering-Balun Configuration

The proposed Minkowski-Like fractal filtering-balun MLFFB is designed based on the dual-mode square ring resonator; as a starting step, see Figure 1. The total perimeter of the closed square ring resonator is responsible for determining the resonant frequency of the proposed MLFFB. In other words, the fundamental resonant frequency occurs when the total length of the perimeter is equal to one wavelength, as well as the harmonics due to the inherent characteristics of the distributed transmission lines. The fractal geometry is applied to each side of the square ring resonator, thereby leading to a design with a compact form. Figure 2 illustrates the process of generation of the proposed MLFFB. As the iteration order n increases, the size of the resonator shrinks symmetrically.

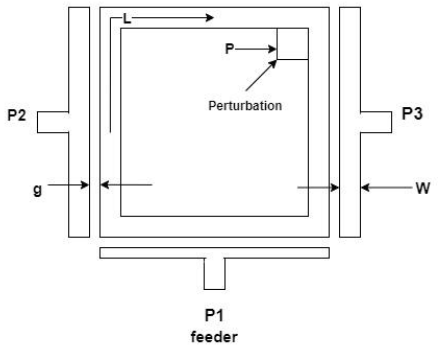

Fig. 1. A schematic layout of the dual-mode ring resonator adopted as a filtering-balun component, where g represents the gap between the feed and resonator, w is the microstrip transmission-line width, L denotes the physical length which is equal to a quarter-wavelength, p is the side length of the square perturbation, and P1, P2, and P3 represent the feeding number.

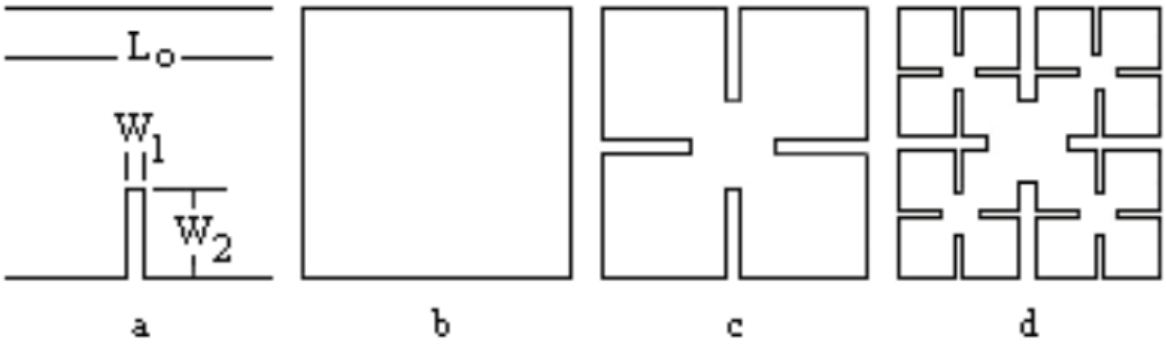

Fig. 2. steps for generating iterations of the Minkowski-like fractal geometry: (a) the generator, (b) the 0th iteration, (c) the 1st iteration, and (d) the 2nd iteration [13].

If the side length of the resonator is fixed, the perimeter Pn will increase when the nth iteration order increases as given by [13]:

$$Pn = \left\{1 + 2\frac{w2}{L0}\right\}(Pn - 1)$$

where w2 and Lo are demonstrated in Figure 2. The Pn goes to infinity, as the iteration order n goes up. This mean that if the total perimeter of the MLFFB keeps unchanged, its area decreases to obtain very small sizes. However, the fabrication technology will considerably be responsible for the highest order we can use due to the limitations of manufacturing.

3 The Filtering-Balun Design

The structure of MLFFB is depicted in Figure 1. It consists of a square-ring resonator with one wavelength in the entire circumference. There is a perturbed stub attached to one of the internal corners, operating to excite the even-odd modes, as will be seen later. There are three ports: one input port and two output ports, or vice versa. The two output ports are balanced (i.e., out-of-phase for each other). In other words, there is a 180° difference in the electrical length between the two output ports. The baluns that will be presented in this paper are good candidates to be utilized with printed dipole antennas since these antennas need a 180o phase difference between the two arms to guarantee that antennas will radiate on the front side (i.e., boresight). If this condition is not satisfied, the radiation null will occur on the front side, while the main grating lobe will be separated into two parts and tilted to move far from boresight [18].

For interested readers, more information about the dual-mode reign resonator analysis is found in [3]. Here, we will go only through the basics for the sake of simplicity. The transmission-line model of the resonator presented in Figure 1 is depicted in Figure 3, where the input and output ports are mentioned. The input signal will be divided equally into two parts. If the perturbation does not exist (i.e., p = 0), there is no output response since each output port collects signals from two paths with a 180° phase difference, canceling each other. To demonstrate the cancellation process, Figure 4 shows the current distribution. The current is at its minimum close to the output ports, so the coupling becomes very weak. However, in the presence of perturbation (i.e., p > 0), the equivalent shunt capacitance Cp acts as a J-inverter, which reverses the phases of the signals passing through it. This helps make the two signals at each output port in-phase, thereby having an output response. Also, the current distribution in this case is displayed in Figure 4. The maxima and minima of the current distribution are rotated by 90°. In other words, the region of coupling between the resonator and the output ports has the maximum current distribution.

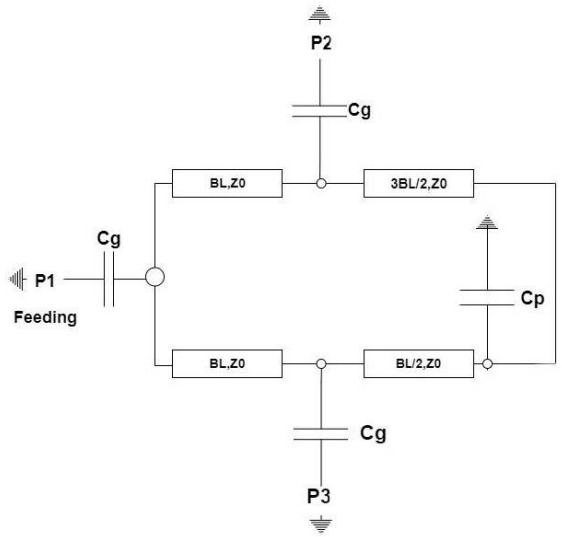

Fig. 3. the transmission line model of the dual-mode square ring filtering-balun component where Cg represents the equivalent capacitance due the gap between the feed and the ring resonator, Cp denotes the equivalent capacitance of the perturbation stub.

4 Results and Discussion

This section presents a thorough discussion about the results obtained from the research. The 0th, 1st, and 2nd iterations of MLFFB are designed, simulated, and analyzed using the full-wave simulation Advanced Design System ADS software. Figure 5 shows the layout schematic of the proposed MLFFBs, and Figure 6 shows their corresponding S-parameters. As can be seen, both output ports have responses that are in line with the brief analysis presented above. To demonstrate the effectiveness of the perturbation size, and only in the case of the 0th iteration of MLFFB, p is changed from 0mm to 6mm with a step of 2mm, as can be seen in Figure 9. The two modes have the same frequency but are out of phase when p = 0 mm, so the S21 and S31 are canceled. For the state p = 2 mm, the modes have almost the same frequency with slight differences, and the two modes have the same phase shift, leading to excitation of S21 and S31. We can say that as p increases, the difference in frequencies between the two modes increases. The center frequency will have a weak response since the phase difference between the two modes increases. All responses in Figure 6 are narrow bands because of the inherent characteristics of the dual-mode ring resonator. It means that these designs will be a good candidate for applications with low noise. As is known, higher bandwidth means higher noise entering the system.

The S21 and S31 are close to -4 dB or -5 dB, although the ideal case should be -3 dB. The extra loss belongs to the fact that the substrate used in this case is lossy, which is the FR4 type. The substrate thickness used in this research is 1.6mm, so some EM waves will be radiated into space, leading to radiation loss. This limitation is due to the substrate availability in the local markets. As a result, for guided RF components such as filters, resonators, transmission lines, etc., substrates with low thicknesses are preferred since the signals will be more tied to the structures and will not leak easily. These two factors have caused the losses in the responses. However, to have better responses, substrates with low losses should be used, especially for commercial purposes. The phase difference between the two output ports for all the proposed MLFFBs is illustrated in Figure 7, where the phase differences are almost equal to 180°.

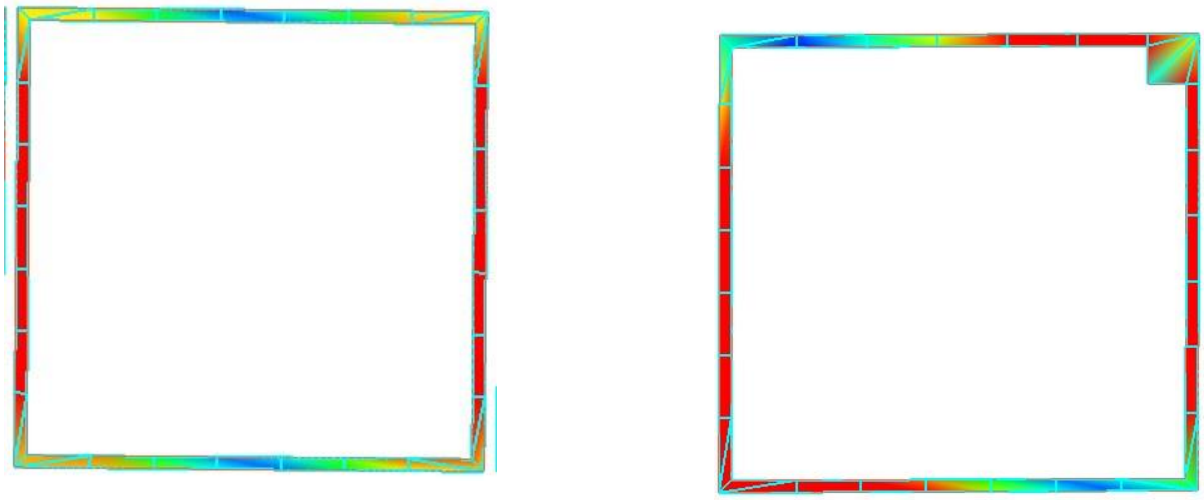

Fig. 4. Simulated current density at the resonance without and with perturbation consecutively.

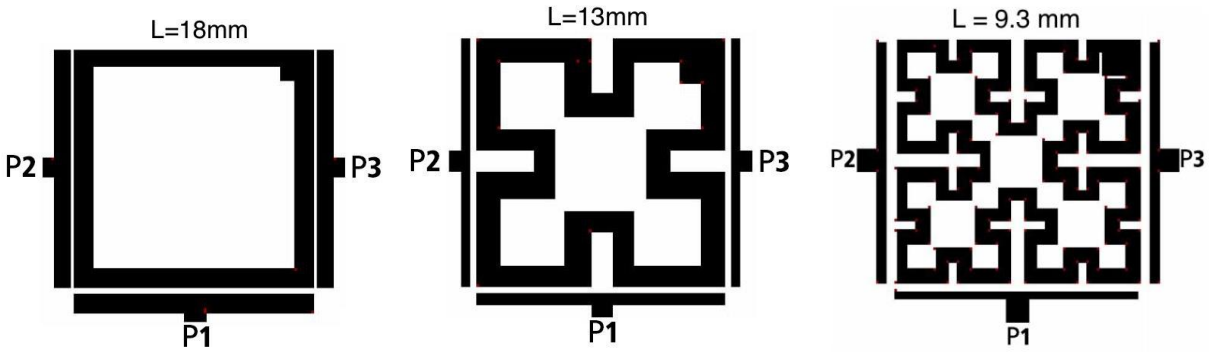

Fig. 5. Layouts of the 0th, 1st, and 2nd iterations of the proposed MLFFBs consecutively

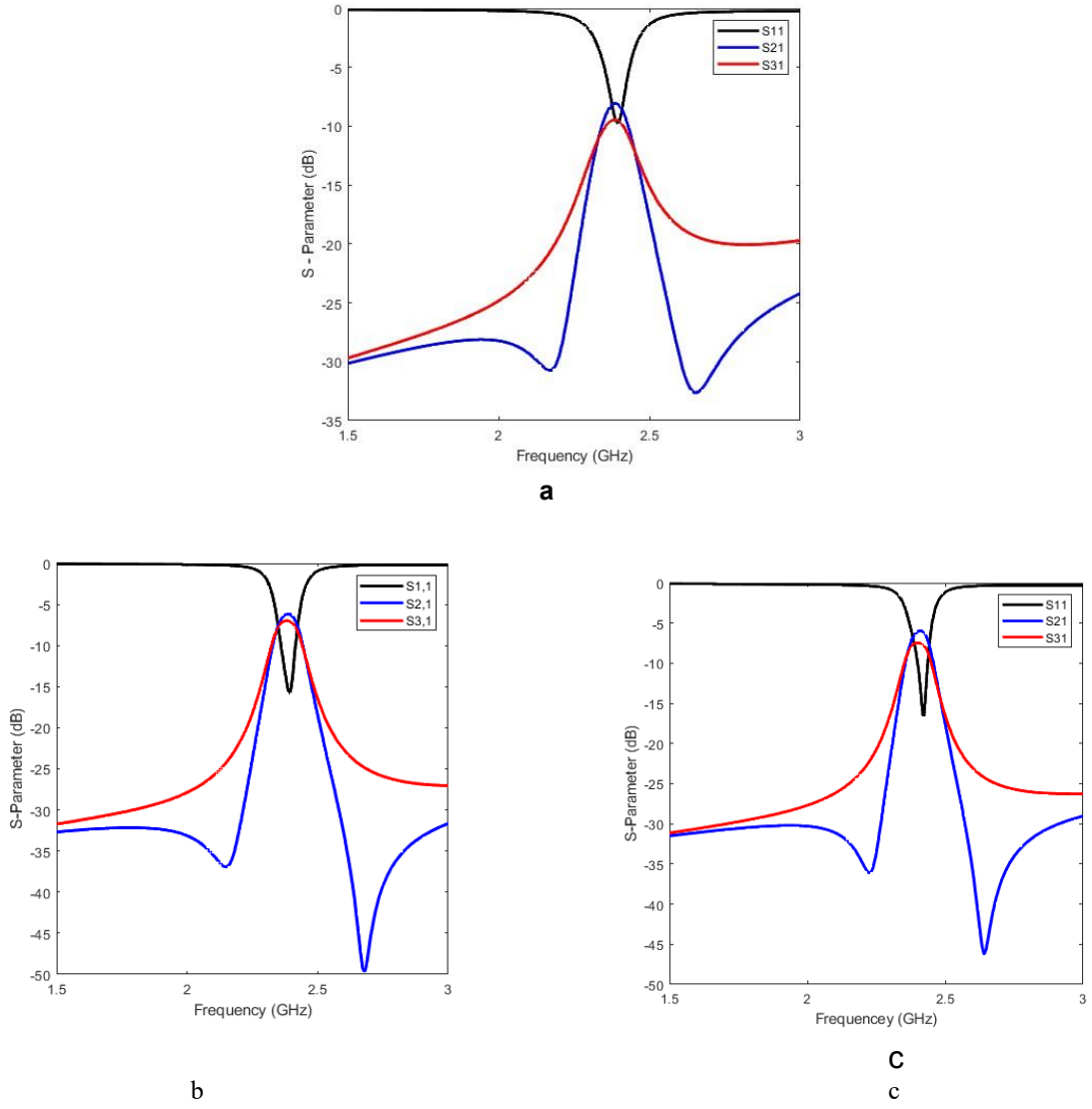

Fig. 6. The S-Parameters responses of the a) 0th, b) 1st, and c) 2nd iterations of the proposed MLFFBs consecutively.

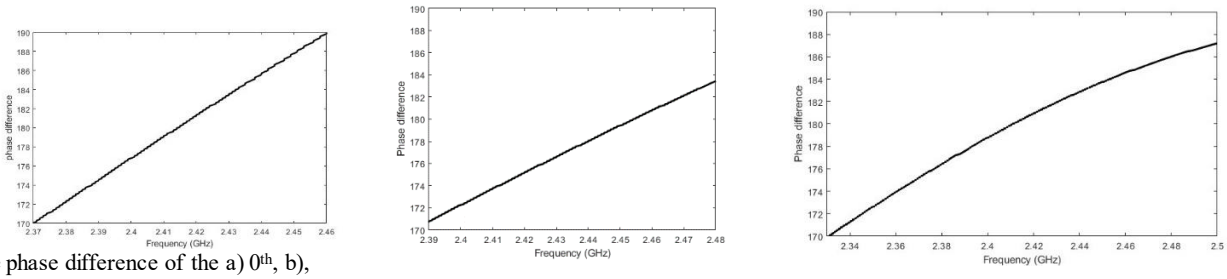

Fig.7. The phase difference of the a) 0th, b), 1st,and c) 2nd iterations of the proposed MLFFBs consecutively

As can be seen, the far output port from the parturition (i.e., port 2) has transmission zeros in the response close the passband, while the near output port (i.e., port 3) has no seen zeros in the response. However, Figure 8 shows a wide range of the transmission response for the 0th iteration of the proposed MLFFB. The first transmission zero of the response occurs after the first harmonic. From Figure 3, the input signal splits into two paths. The path associated with the output port 2 has an extra electrical distance equal to $3\beta L/2$ to reach the perturbation stub, while the path associated with the output port 3 has an extra electrical distance equal to $\beta L/2$ to reach the perturbation stub. The perturbation considers as a virtual ground at high frequencies, so the two paths can have independent paths. The longer path will resonate at lower frequency to ground the signals, considered as a transmission zero, but the shorter path will resonate at higher frenemies. Since the shorter path is less by three times, so the first transmission zero of the third output port occurs at a frequency three times more. This investigation is ideal, but because of coupling, the transmission will occur lower or higher by a ratio depending on the design structure. Also, the perturbation size changes the total electrical length, thereby the transmission zero will occur earlier.

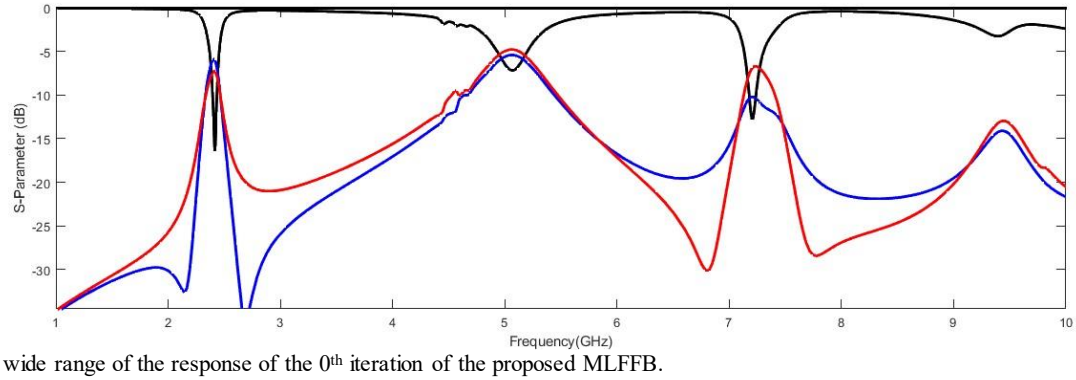

Fig. 8. A wide range of the response of the 0th iteration of the proposed MLFFB.

To demonstrate how the perturbation size affects the response and the location of the transmission zeroes, see Figure 9. Next, amplitude imbalances, and phase errors of all presented iterations of the MLFFB are introduced in Figure 10. As the response moves away from the design frequency, these three parameters vary, leaving the optimal values. This occurs because the designs are made of transmission lines where they are dispersive. In other words, when the frequency changes, the equivalent electrical length changes as well. Therefore, the design response deviates from its determined value. Figure 11 shows the current distributions for the 2nd iteration of the proposed MLFFB at 2Gz, 2,45GHz and 3GHz consecutively to demonstrate the properties of bandpass filters. Figure 12 shows the distributed electrical current, and as can be seen that the direction of arrows is completely reversed at the output ports as an evident to obtain a structure with a balun characteristic. More details can be found in [19].
Finally, Table 1 shows the miniaturization ratio obtained for the 1st and 2nd iterations of the proposed MLFFBs compared to the 0th iteration one. As expected, as an iteration order n increases, the designs with smaller footprint are realized. More than 80% miniaturization ratio is obtained for the 2nd iteration MLFFB. For multifunctional wireless low power devices, smaller components are highly needed to realize the systems with a reasonable size.

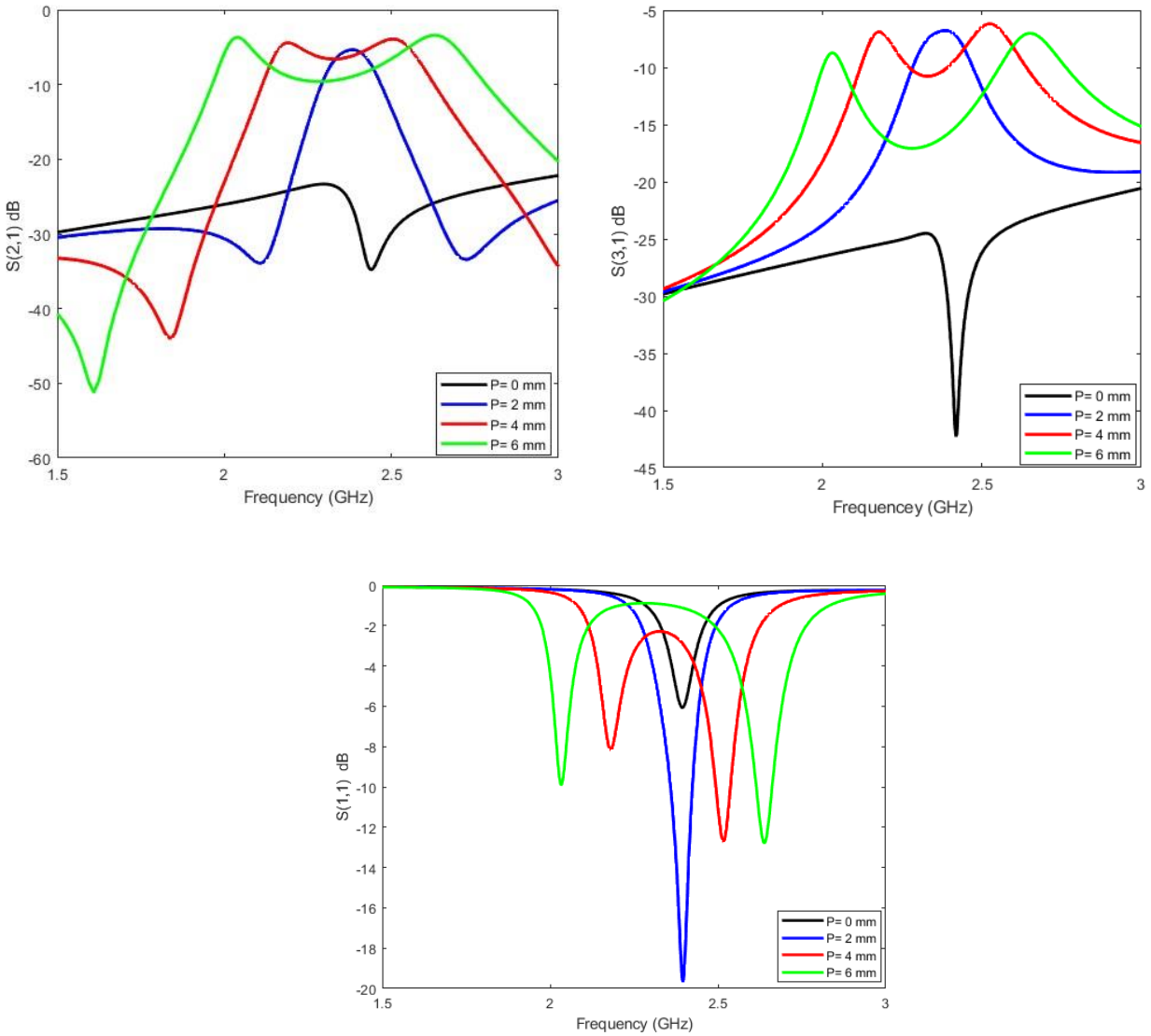

Fig. 9: The S-parameters responses S21, S31 and S11 of the 0th iteration of the MLFFB consecutively, when p is changed from 0mm to 6mm with a step of 2mm.

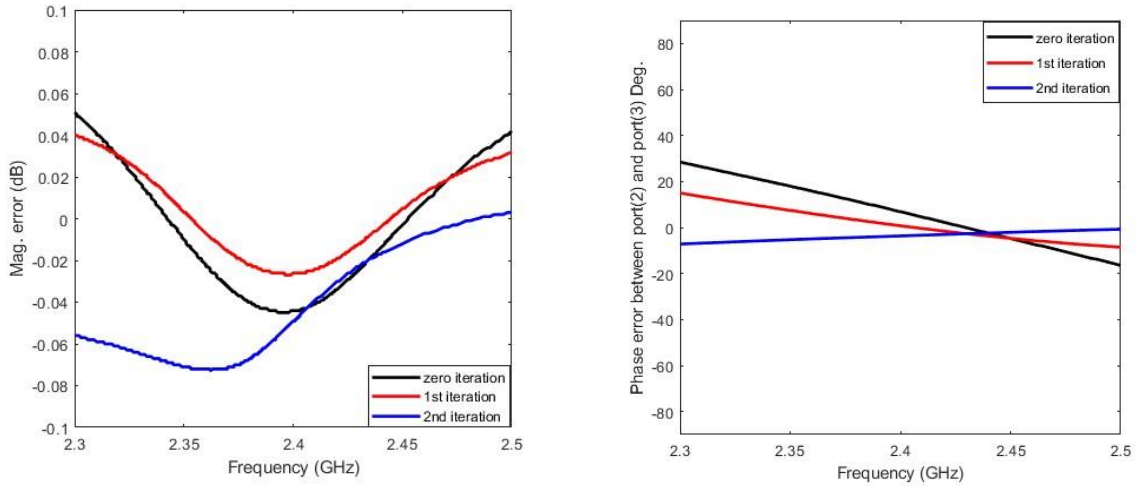

Fig. 10. Magnitude imbalance and phase errors of the 0th, 1st, and 2nd iterations of the proposed MLFFBs.

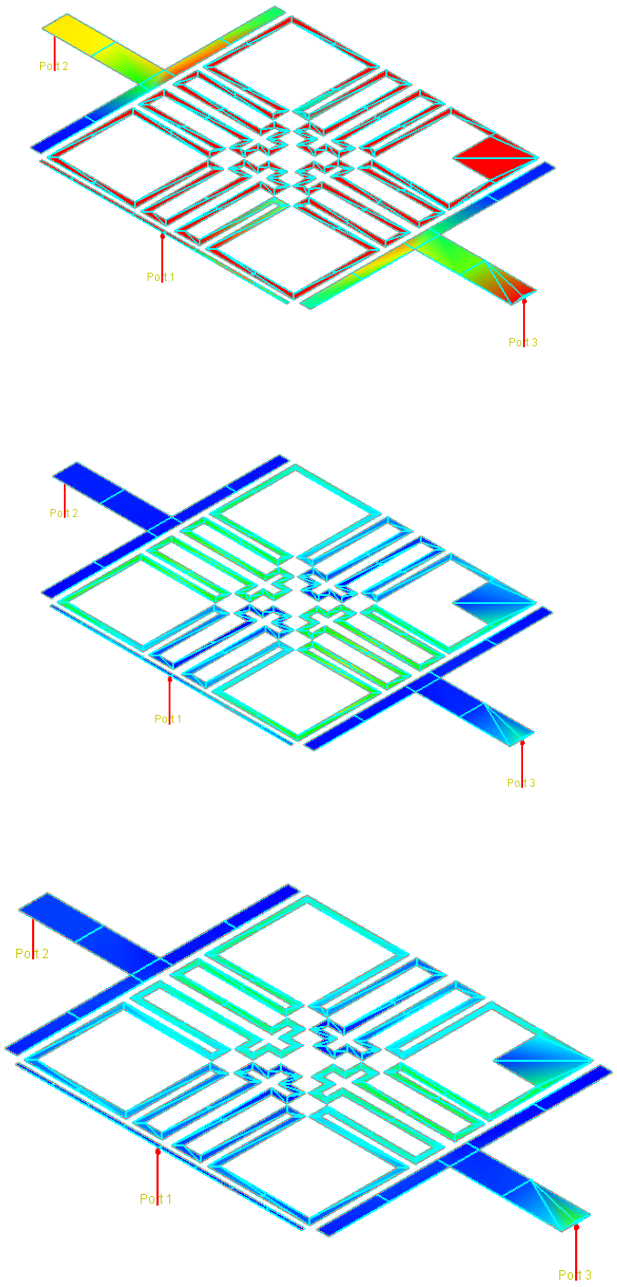

Fig. 11. Current distributions of the 2nd iteration of the MLFFB at 2GHz, 2.45 GHz, and 3GHz consecutively.

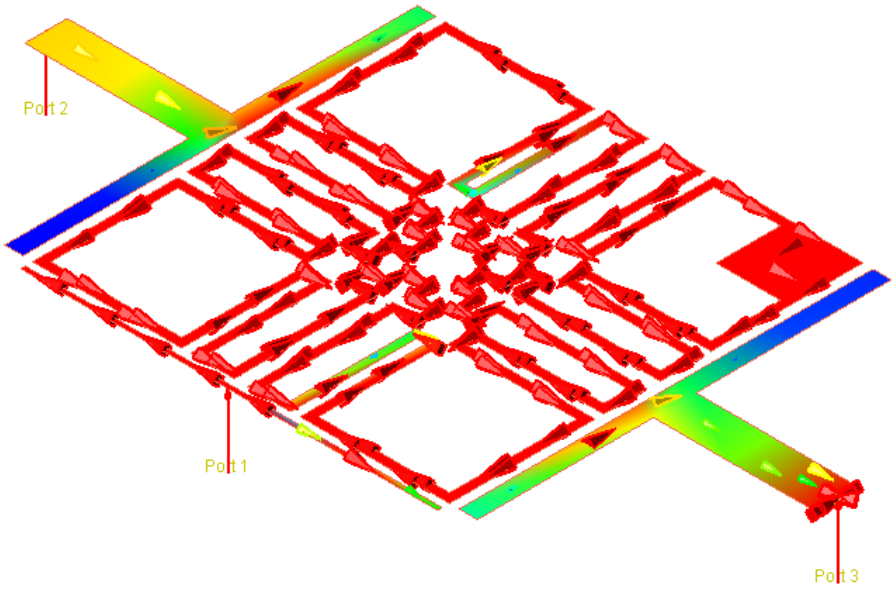

Fig. 12. Current distributions of the 2nd iteration of the MLFFB at 2.45 GHz showing the directions of currents at the output port.

Table 1. the side length and the miniaturization ratios of the proposed MLFFB compared with the 0th iteration one.

The iteration number n	Side length of square resonator	Reduction ratio
Zero	18 mm	----
1st	13 mm	47.8 %
2nd	9.3 mm	73 %

6 Conclusion

In this research, the dual-mode ring resonator based on miniaturized fractal balun-filtering was presented for the first time according to the best of the authors' knowledge. The input signals were divided into two outputs that were out of phase, making them a good candidate for applications operating with two balanced input ports, especially the dipole antenna. An FR4 substrate with a thickness of 1.6mm was used in the research. Its impact was obvious on the S21 and S31, which were close to -4 to -5 dB, related to the 0th iteration of the MLFFB, the miniaturization ratios of the 1st and 2nd iterations were 47.8% and 73%, respectively. Moreover, a theoretical brief of the analysis with an accompanying equivalent circuit was provided to give the readers almost a complete idea of the design. Several parameters have been visualized, such as current distributions, phase differences, phase errors, and magnitude imbalances. All presented designs had few phase errors and magnitude imbalances near the operating frequencies.

References

1. J. S. Hong and M. J. Lancaster, "Bandpass characteristics of new dual-mode microstrip square loop resonators," Electron. Lett., vol. 31, no. 11, pp. 891–892, May 1995.
2. J. S. Hong and M. J. Lancaster, "Microstrip bandpass filter using degenerate modes of a novel meander loop resonator," IEEE Microwave Guided Wave Lett., vol. 5, pp. 371–372, Nov. 1995.
3. A Gorur, "Description of coupling between degenerate modes of a dual-mode microstrip loop resonator using a novel perturbation arrangement and its dual-mode bandpass filter applications,"

in *IEEE Transactions on Microwave Theory and Techniques*, vol. 52, no. 2, pp. 671-677, Feb. 2004, doi: 10.1109/TMTT.2003.822033

4. E. -Y. Jung and H. -Y. Hwang, "A Balun-BPF Using a Dual Mode Ring Resonator," in *IEEE Microwave and Wireless Components Letters*, vol. 17, no. 9, pp. 652-654, Sept. 2007,
5. P. Cheong, T. -S. Lv, W. -W. Choi and K. -W. Tam, "A Compact Microstrip Square-Loop Dual-Mode Balun-Bandpass Filter With Simultaneous Spurious Response Suppression and Differential Performance Improvement," in *IEEE Microwave and Wireless Components Letters*, vol. 21, no. 2, pp. 77-79, Feb. 2011,
6. M. M. Bajestan, V. D. Rezaei and K. Entesari, "A 2.75–6.25GHz low-phase-noise quadrature VCO based on a dual-mode ring resonator in 65nm CMOS," *2014 IEEE Radio Frequency Integrated Circuits Symposium*, Tampa, FL, USA, 2014, pp. 265-268, doi: 10.1109/RFIC.2014.6851715.
7. Passaro, V.M.N.; Tullio, C.D.; Troia, B.; Notte, M.L.; Giannoccaro, G.; Leonardis, F.D. Recent Advances in Integrated Photonic Sensors. *Sensors* **2012**, *12*, 15558-15598. https://doi.org/10.3390/s121115558
8. Passaro, V.M.N.; Troia, B.; La Notte, M.; De Leonardis, F. Chemical Sensors Based on Photonic Structures. In *Advances in Chemical Sensors*; Wang, W., Ed.; InTech: Rijeka, Croatia, 2012. [**Google Scholar**]
9. Air Mohammad Siddiky, Mohammad Rashed Iqbal Faruque, Mohammad Tariqul Islam, Sabirin Abdullah, A multi-split based square split ring resonator for multiband satellite applications with high effective medium ratio, Results in Physics, Volume 22, 2021, 103865, ISSN 2211-3797, https://doi.org/10.1016/j.rinp.2021.103865.
10. Wang, Ben-Xin, et al. "A broadband terahertz metamaterial absorber enabled by the simple design of a rectangular-shaped resonator with an elongated slot." *Nanoscale Advances* 1.9 (2019): 3621-3625.
11. D. G. Rabus, M. Hamacher, U. Troppenz and H. Heidrich, "Optical filters based on ring resonators with integrated semiconductor optical amplifiers in GaInAsP-InP," in *IEEE Journal of Selected Topics in Quantum Electronics*, vol. 8, no. 6, pp. 1405-1411, Nov.-Dec. 2002, doi: 10.1109/JSTQE.2002.806692.
12.
13. Wang, Chunlei, and Kai Chang. "Microstrip multiplexer with four channels for broadband system applications." *International Journal of RF and Microwave Computer-Aided Engineering: Co-sponsored by the Center for Advanced Manufacturing and Packaging of Microwave, Optical, and Digital Electronics (CAMPmode) at the University of Colorado at Boulder* 11.1 (2001): 48-54.
14.
15. Ali, Jawad K., and Nasr N. Hussain. "An extra reduced size dual-mode bandpass filter for wireless communication systems." *Proc. Progress in Electromagnetics Research Symp., PIERS*. 2011.
16. Ali, Jawad K., and N. N. Husain. "A new fractal microstrip bandpass filter design based on dual-mode square ring resonator for wireless communication systems." *Iraqi Journal of Applied Physics* 5.1 (2009).
17. Ahmed, Hayder S., et al. "A compact triple band BSF design based on Minkowski fractal Geometry." *2016 18th Mediterranean Electrotechnical Conference (MELECON)*. IEEE, 2016.
18. Xu, He-Xiu, Wang, Guang-Ming, Lu, Ke and Chen, Xin. "Fractal-Shaped Balun Using Composite Right/Left-Handed Transmission Line for Bandwidth Enhancement" *Frequenz*, vol. 65, no. 5-6, 2011, pp. 121-126. https://doi.org/10.1515/freq.2011.019
19. H. -X. Xu, G. -M. Wang, X. Chen and T. -P. Li, "Broadband Balun Using Fully Artificial Fractal-Shaped Composite Right/Left Handed Transmission Line," in *IEEE Microwave and Wireless Components Letters*, vol. 22, no. 1, pp. 16-18, Jan. 2012, doi: 10.1109/LMWC.2011.2173929.
20. Yongxi Qian, W. R. Deal, N. Kaneda and T. Itoh, "A uniplanar quasi-Yagi antenna with wide bandwidth and low mutual coupling characteristics," *IEEE Antennas and Propagation Society International Symposium. 1999 Digest. Held in conjunction with: USNC/URSI National Radio Science Meeting (Cat. No.99CH37010)*, Orlando, FL, USA, 1999, pp. 924-927 vol.2, doi: 10.1109/APS.1999.789463.
21. Pozar, David M. *Microwave engineering*. John wiley & sons, 2011.